

## THE HYDROGEN ADSORPTION BEHAVIOR OF MECHANO-CHEMICALLY ACTIVATED CARBON FROM INDONESIAN LOW-RANK COAL: COUPLED LANGMUIR AND DUBININ-ASTAKHOV ISOTHERM MODEL ANALYSIS

Sri Harjanto<sup>1</sup>, Jaka Fajar Fatriansyah<sup>1\*</sup>, Latifa Nuraini Noviana<sup>1</sup>, Stefano Widy Yuniior<sup>1</sup>

<sup>1</sup>*Department of Metallurgy and Materials Engineering, Faculty of Engineering, Universitas Indonesia, Kampus UI Depok, Depok 16424, Indonesia*

(Received: May 2018 / Revised: June 2018 / Accepted: July 2018)

### ABSTRACT

This study aims to produce activated carbon from low-rank coal from East Kalimantan, Indonesia by a mechano-chemical method and to determine its adsorption parameters: hydrogen uptake/capacity, activation energy, the structural heterogeneity parameter, and the isosteric heat of adsorption. The hydrogen uptake/capacity of the coal was determined by a volumetric adsorption test using constant-volume-variable-pressure (CVVP). The characteristic adsorption parameters, such as hydrogen uptake, characteristic energy and heterogeneity structure factor, were determined using the coupled Langmuir and Dubinin-Astakhov (D-A) isotherm models, with the assumption that the hydrogen uptake value would be similar, irrespective of the model used. We found that the mechano-chemical method significantly reduced the particle size of the activated carbon relative to the untreated control, by approximately 60%. In addition, the activation process yielded a higher surface area for the activated carbon (390 m<sup>2</sup>/g) compared to the untreated control (90 m<sup>2</sup>/g). We also found that greater surface area led to a greater uptake of hydrogen by the activated carbon (40.17±1.56)×10<sup>-3</sup> kg/kg than by the untreated control (7.94±1.56)×10<sup>-3</sup> kg/kg. We also found that the heterogeneity factor of the activated carbon was 3.73±0.23, lower than the untreated control 4.65±0.56, which reflects the more heterogeneous pore diameter sizes for the activated carbon compared to the untreated control. Lastly, using the obtained adsorption parameters, we observed that the hydrogen uptake-dependent isosteric heat of adsorption on the activated carbon changed rapidly in the initial and final stages compared to the untreated control due to the adsorption of hydrogen by smaller pores which reside inside larger ones.

**Keywords:** Activated carbon; Adsorption isotherms; Heterogeneity; Planetary ball mill; Sub-bituminous coal

### 1. INTRODUCTION

Hydrogen is an ideal future fuel source. For example, it can be utilized in combustion to produce water, which does not contribute to air pollution (Serrano et al., 2009; Jiménez et al., 2010; Nasruddin et al., 2016). In fuel cell applications, hydrogen is directly converted into water, electricity and heat. Therefore, the use of hydrogen as an energy source may possibly reduce harmful emissions of greenhouse gases (such as carbon dioxide, carbon monoxide, hydrocarbons, nitrogen oxides, and sulphur oxides), and may reduce global dependence on fossil fuels, especially in the transportation sector. For hydrogen to be properly used as

---

\*Corresponding author's email: fajar@metal.ui.ac.id, Tel. +62-21-7863510, Fax. +62-21-7872350  
Permalink/DOI: <https://doi.org/10.14716/ijtech.v9i5.2031>

an energy source, an effective storage medium is needed. The required properties of a hydrogen storage medium are that it should be low in weight, low in price, easy to activate and have good availability, high volumetric and gravimetric hydrogen density, and long-term cycle stability (Niemann et al., 2008). Some examples of hydrogen storage materials are carbon-based ones such as activated carbon (Marsh et al., 1984) and graphite nanofiber (Chambers et al., 1998), and other materials such as metal organic frameworks (Li et al., 1999), zeolites (Dong et al., 2007), clathrate hydrates (Lee et al., 2005) and metal hydride (Schlapbach & Züttel, 2001).

Activated carbon is an appropriate choice for a hydrogen storage medium due to its high porosity (Nor et al., 2016), low bulk density (Caturla et al., 1991), reasonable cost (El Qada et al., 2006), relative abundance, and capability to store gases on its surface (De la Casa-Lillo et al., 2002). It can be produced from carbon-rich materials such as coal and various agricultural residues (Ioannidou & Zabaniotou, 2007). Among these, coal has the greatest potential as a carbon-containing material because it is relatively abundant and economical. Further, the production of activated carbon from coal can increase its commercial value.

Basically, activated carbon can be produced by two methods: by chemical activation (Marsh et al., 1984; Kumamoto et al., 1994; Ahmadpour & Do, 1997; Tsai et al., 1998) or by physical activation (Caturla et al., 1991; Ahmadpour & Do, 1996; Bouchelta et al., 2008; Nandi et al., 2012; Sekirifa et al., 2013). In this study, we develop a combination of physical/mechanical and chemical methods, known as the mechano-chemical method, to produce activated carbon by means of a planetary ball mill and with KOH introduced. Mechanically-driven activation is induced by imposing a mechanical force on a material, and chemical activation is induced by reacting a chemical compound with the material. We expect that the combination will produce activated carbon which has good characteristic adsorption parameters.

Several models have been developed to characterize gas adsorption in microporous materials (Do, 1998). Among them, the Dubinin-Astakhov (D-A) model is well known for its characterization of the non-homogeneous structure of microporous materials. In this model, some parameters can be revealed to evaluate the gas adsorption characteristics of microporous materials, such as carbon-based ones. Several previous studies have examined the D-A model to characterize the adsorption behaviour of multiple gas species on activated carbon materials (Hu & Ruckenstein, 2006; Ushiki et al., 2013; Wu et al., 2014) and have determined that it is applicable for such a purpose.

This study aims to produce activated carbon from Indonesian low-rank coal by a mechano-chemical method and to determine its adsorption parameters: hydrogen uptake/capacity, activation energy, the structural heterogeneity parameter, and the isosteric heat of adsorption. The volumetric method-based experiment was designed to determine the adsorption parameters, and two simultaneous isotherm methods—the Langmuir and D-A methods—were coupled to calculate the adsorption parameters properly. Further, the parameters obtained from the calculation can be used to predict the mechanism of hydrogen adsorption on the activated carbon surface.

## 2. GAS ADSORPTION MODELS

The Langmuir and D-A models were both employed to determine the isosteric heat of adsorption. The Langmuir model is used to describe monolayer adsorption phenomena in a microporous solid, assuming that the adsorbent surface is homogenous. The adsorption on the surface is localized, with each site only being able to accommodate a single molecule. Thus, the adsorption energy is constant at all sites. Because the study focuses on an average value of the thermo-physical parameters, this model is appropriate for the system examined here. The Langmuir model can be written as (Dubinin, 1975):

$$\frac{C}{C_0} = \frac{k_0 \exp(h_{st}/RT)P}{1 + k_0 \exp(h_{st}/RT)P} \quad (1)$$

where  $C_0$  is the hydrogen/gas uptake or the saturated amount of the adsorbed gas,  $k_0$  is the equilibrium constant,  $h_{st}$  is the isosteric heat of adsorption,  $T$  is the temperature (K),  $P$  is the equilibrium pressure (Pa), and  $R$  is the gas constant. Equation 1 can be used directly to fit the experimental results. Sudibandriyo et al. (2015) employed the Langmuir model to analyze hydrogen adsorption data in order to determine the adsorption capacity of carbon nanotubes used as hydrogen storage.

The D-A model of micropore volume postulates that the gas adsorption mechanism in micropores is a porosity filling mechanism (Dubinin, 1975). Accordingly, to describe the adsorption process correctly, the heterogeneity of the solid surface, which is related to the energetics, should be considered (Gil & Korili, 2000). The heterogeneity of the surface can originate from crystal and geometric irregularities which exist on the solid surface (Jaroniec, 1995). Commonly, the heterogeneity is measured by relating the distribution gradient of multiple adsorption sites to the adsorption energy. The distribution function used is a Gaussian-like function which expresses the distribution of pore sizes. The generalized D-A model can be written as follows (Dubinin, 1975):

$$C = C_0 \sum_{i=1}^m f_i \exp \left[ - \left( \frac{A}{E} \right)^n \right] \quad (2)$$

where  $f_i$  is the local fraction of the adsorption sites (Dubinin, 1975).

$$A = -\Delta G = RT \ln \left( \frac{P_0}{P} \right) \quad (3)$$

is the adsorption potential of the Polanyi theory, which is related to the change in the Gibbs free energy  $\Delta G$ . The change in the relative pressure  $\frac{P_0}{P}$ ,  $E$  is the characteristic energy of the adsorption system, and  $n$  is the structural heterogeneity parameter, which is linked to the adsorption of structurally heterogeneous solids. Lower values of  $n$  indicate greater heterogeneity than that of higher values.  $P_s = (T/T_c)^2 P_c$  (for  $T > T_c$ ) is the saturation pressure, with  $P_c$  and  $T_c$  being the critical pressure and temperature, respectively. In contrast to the Langmuir model, the D-A model considers the structural heterogeneity of the adsorbent. Equation 2 relates the summation of multiple isotherms which have different characteristic energies to a specific pore-group distribution. In fact, this model is very suitable for describing adsorption in highly activated carbon (Stoeckli et al., 1994). However, in order to be coupled to the Langmuir model, the D-A model needs to be simplified, assuming that a single distribution of pores exists related to only one characteristic energy. In this way, it is possible to couple the equations, assuming that the outcome of  $C_0$  for both models is similar. Therefore, the simplified D-A equation can be written as follows (Dubinin, 1975):

$$C = C_0 \exp \left[ - \left( \frac{A}{E} \right)^n \right] \quad (4)$$

where  $C$  is the adsorption potential,  $E$  is the adsorption system characteristic energy, and  $n$  is a parameter of structural heterogeneity.  $P_s = \left(\frac{T}{T_c}\right)^2 P_c$  (for  $T > T_c$ ) is the saturation pressure, and  $P_c$  and  $T_c$  are the critical pressure and temperature, respectively. In contrast to the Langmuir model, the D-A model considers the structural heterogeneity of the adsorbent. Here, to make fitting more convenient, the D-A model (Equation 2) can be reformulated as (Dubinin, 1975):

$$\ln \left[ \ln \left( \frac{C_0}{C} \right) \right] = n \ln \left[ \frac{RT}{E} \ln \left( \frac{P_s}{P} \right) \right] \quad (5)$$

The heat which evolves during the adsorption process or the isosteric adsorption heat ( $h_{st}$ ) can be calculated from the Chakraborty derivation (Chakraborty et al., 2006) and is written as follows:

$$h_{st} = 2RT + E \left( \frac{C_0}{C} \right)^{1/n} + T v_g \frac{dP}{dT} (P, T) \quad (6)$$

where  $v_g$  is the vapor phase specific volume.

### 3. METHODS

#### 3.1. Materials

The raw material for the activated carbon was untreated low-rank coal obtained in January 2013 from coal mines in East Kalimantan, Indonesia. This was crushed to obtain micrometer-sized particles (<150  $\mu\text{m}$ ). After crushing, the carbonization process was conducted at a temperature of 973 K for around 60 minutes in an inert furnace. At this point, the sample was ready to be activated using the mechano-chemical method. This method is composed of two basic activation processes: chemical and mechanical activation (see Figure 1).

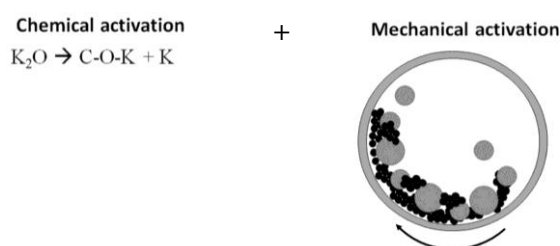


Figure 1 Schematic illustration of the novel mechano-chemical activation method, using planetary ball milling and addition of KOH

The first activation was the chemical activation using KOH, which produces potassium (Moreno-Castilla et al., 2001). This activation was conducted by mixing the carbonized coal with KOH at a weight ratio of 1:4, which is the optimum ratio required to promote the highest surface areas at reaction temperatures below 1073 K (Marsh et al., 1984).  $\text{K}_2\text{CO}_3$  might be formed during the process, which will then be decomposed to  $\text{K}_2\text{O}$  and  $\text{CO}_2$ . In the carbon-rich environment, a reduction reaction may take place to produce potassium (Figure 1). The next process was mechanical activation. In this process, the mixed coal was milled inside a planetary ball mill NQM-4 in dry conditions for around 4 hours, with a rotation speed of 200 rpms. The diameters of the planetary balls were in the range from 5 to 20 mm, with the ratio between the sample and planetary ball weight being 1:5. After milling, the coal was then heated at a temperature of 1023 K for around 75 minutes in the inert furnace and was then washed using 5

M HCl and distilled water. The samples were dried again at 120°C for about 4 hours. The final products were called activated carbon.

The composition of the untreated low-rank carbon is shown in Table 1. This composition was obtained from proximate analysis in accordance with the ASTM D 121 standard. The untreated coal can be categorized as sub-bituminous coal, which contains a low fraction of fixed carbon (Ahn et al., 2001). The Brunauer Emmett Teller (BET) test (quantachrome NOVA 1200e Surface Area & Pore Size Analyzer) was conducted to measure the surface area, pore size and pore volume of the samples (untreated coal and activated coal) using nitrogen gas. X-ray diffractometer characterization was made by an XRD instrument Shimadzu Maxima 7000, while microstructure characterization of the samples was made using a Scanning Electron Microscope (SEM, FEI INSPECT F50).

Table 1 Composition of the untreated Indonesian low-rank coal

Proximate Analysis	
Moisture	11.71 %
Ash	2.70 %
Volatile Matter	39.86 %
Fixed Carbon	45.73 %

### 3.2. Apparatus and Procedure

The hydrogen uptake of the coals was determined by a volumetric adsorption test. The pressure drop due to the adsorption of hydrogen by the samples was measured, and the hydrogen uptake investigation was conducted using constant-volume-variable-pressure (CVVP).

Figure 2 shows a schematic diagram of the experimental apparatus used in the study; it is similar to that used in previous works (Martin et al., 2011; Harjanto et al., 2013). The apparatus consisted of two cylinders: a charging cylinder made of stainless steel (SS 304) and a measuring cylinder, with volumes of 1118 ml and 80.8 ml respectively. The cylinders were connected by a stainless steel tube immersed in a temperature-controlled fluid bath, in which temperature fluctuation was kept below  $\pm 0.1$  K. The pressure was measured using an absolute pressure transmitter (DRUCK PTX 1400) with a range of 0 to 40 bar and 0.15% accuracy. Temperature is measured by a Class-A Type K thermocouple. The measurement data were acquired using a National Instrument data logger.

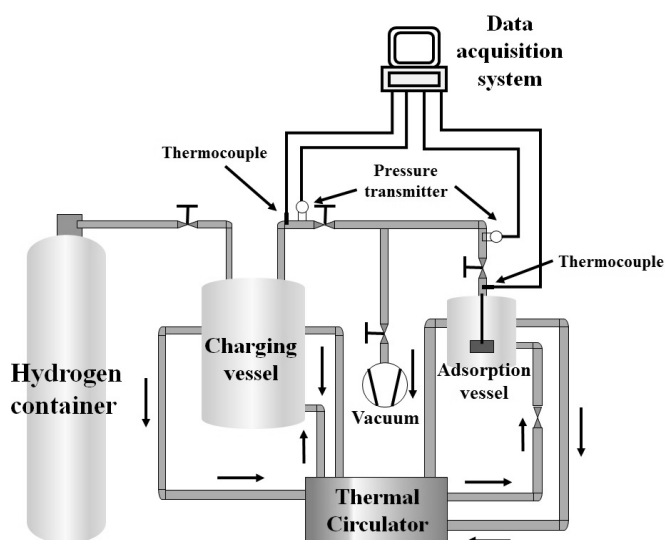


Figure 2 Schematic diagram of the experimental apparatus

Prior to the isotherm test (at a constant temperature), a degassing process was conducted for around 8 hours to ensure that there was no substance or impurity contamination in the measurement system. After isothermal conditions were attained, hydrogen was pumped into into the charging cell. The pressure varied by up to 4 MPa. This process was repeated for different temperatures. The variable obtained from the experiment was the pressure-dependent hydrogen uptake  $C$ , which is the ratio of the amount of adsorbed gas to the mass of adsorbent.

The Langmuir and D-A models were coupled and used to fit the experimental data simultaneously. They were then analyzed to capture the heterogeneity of the activated carbon adsorbents and to predict the mechanism of hydrogen adsorption in the activated carbon produced.

#### 4. RESULTS AND DISCUSSION

##### 4.1. Physical Properties and Microstructure of the Activated Carbon

The physical properties are attributed to the product of the ball-mill mechano-chemical activation method. A shift in particle size distribution to smaller diameters was observed after the mechano-chemical treatment (see Figure 3). The particle size distribution of the milled samples fell by around 60%, from their average size of 55  $\mu\text{m}$  to 22  $\mu\text{m}$ . This indicates that the mechano-chemical method can significantly reduce the particle size of the samples. Consequently, this method also contributes to the transformation of other physical properties, as listed in Table 2.

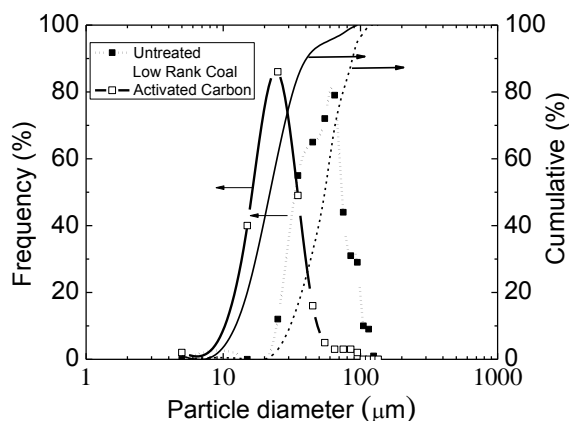


Figure 3 Particle size distribution of the raw material (untreated low-rank coal) and activated carbon after mechano-chemical treatment

Several physical properties of the activated carbon were compared with the untreated coal; these are listed in Table 2. Its micropore volume increased more than two-fold compared to the untreated coal. This result also shows that the surface area increased more than 400% compared to that of untreated coal. The treatment method decreased the pore size slightly, from 1.89 nm of the untreated coal, to 1.15 nm of the activated carbon. The mechanical/physical procedure, the ball milling, results in an increase in BET surface, as previously shown by Baheti et al. (2015), whose activated carbon surface area almost doubled. However, this is not always the case. Welham et al. (2002) showed that physical activation does not translate into an increase in surface area; in their case, this decreased after ball mill physical activation. The chemical activation by KOH, as reported by Ahmadpour and Do (1997), only increased the surface area by 20 to 30%. In our study, the combination of the physical (ball mill) and chemical (KOH) increased the carbon surface area more than three-fold.

Viswanathan et al. (2009) showed that the potassium created in chemical activation intercalates into lamellae of the crystallite. However, in our experiment the washing by HCl removed the potassium, thus increasing porosity and carbon surface area. The XRD results in Figure 4 show that no peaks of potassium hydroxide were detected.

Table 2 Physical properties of untreated low-rank carbon and activated carbon determined using Brunauer Emmett Teller (BET)

Analysis parameter	Untreated low-rank coal	Activated carbon
Micropore volume (l/kg)	0.085	0.23
Surface area (m <sup>2</sup> /g)	90	390
Pore size diameter (nm)	1.89	1.15

Figure 5a shows secondary images of the microstructure of the untreated sample, while Figure 5b shows that of the activated sample. It can be observed that the activated carbon contains abundant pores. In general, these can be classified as macropores, mesopores and micropores, which have diameters of more than 400 nm, 2–400 nm and less than 2 nm, respectively (Dubinin 1975). Figure 5b shows porosity which can be classified as macropores on the surface of the activated carbon. Other smaller porosities inside the macropores are shown in the Figure 5b. The existence of mesopores and micropores on the surface and/or inside the macropores can be expected, although they cannot be observed clearly.

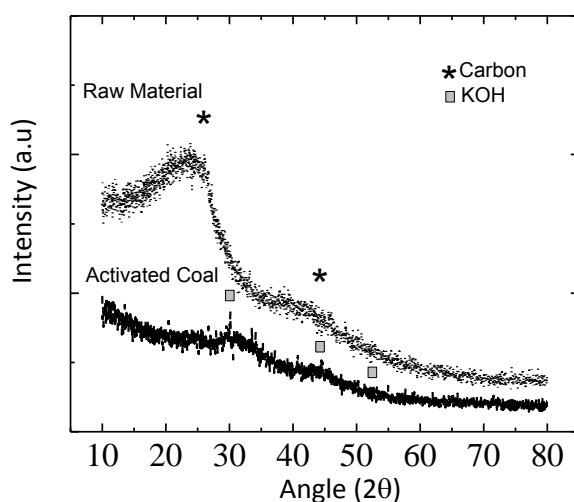


Figure 4 XRD pattern of the raw material and activated carbon from coal

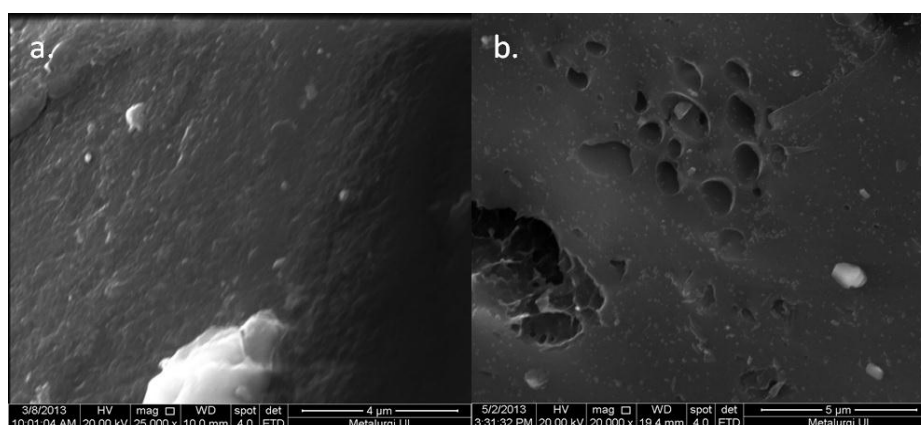


Figure 5 Secondary images of the sample microstructure: (a) untreated low-rank coal; (b) activated carbon. Abundant macropores are observed in (b)

### 4.2. Hydrogen Adsorption Parameters

It was expected that the hydrogen uptake, or the saturated amount of the adsorbed gas (hydrogen) of the activated carbon  $C_0$ , would be higher than that of the untreated coal due to the increase in pore volume and surface area, which leads to a higher amount of hydrogen that can be adsorbed by the material. To determine the value of  $C_0$ , the adsorption experiment results were fitted to both models. Figure 6 shows the adsorption experiments which were conducted at temperatures of 268 K, 283 K and 298 K for activated carbon (298 K for untreated coal, see Figure 6a) and pressures of up to 4 MPa.

According to the Langmuir model, there is a saturation value or plateau of hydrogen uptake when the system reaches high pressure, depending on the adsorbate gas and adsorption surface. Our system can be categorized as an “L type” of isotherm, which is the characterization of non-solid adsorption on the solid surface (Limousin et al., 2007). The trend of the curve shows the progressive saturation of the solid. In other words, physically the adsorbent reaches its capacity to adsorb the surrounding gas. It can be clearly seen that in Equation 1, if one takes the limit, where  $P \rightarrow \infty$ , then we get  $C \rightarrow C_0$ . However, from the experimental results obtained (see Figure 5b), one can see that only a linear relationship between hydrogen uptake and pressure is observed. Our apparatus can only produce pressure up to 4000 kPa. Therefore, to avoid obtaining incorrect fitting parameters, the data were also fitted using the D-A model and both models coupled.

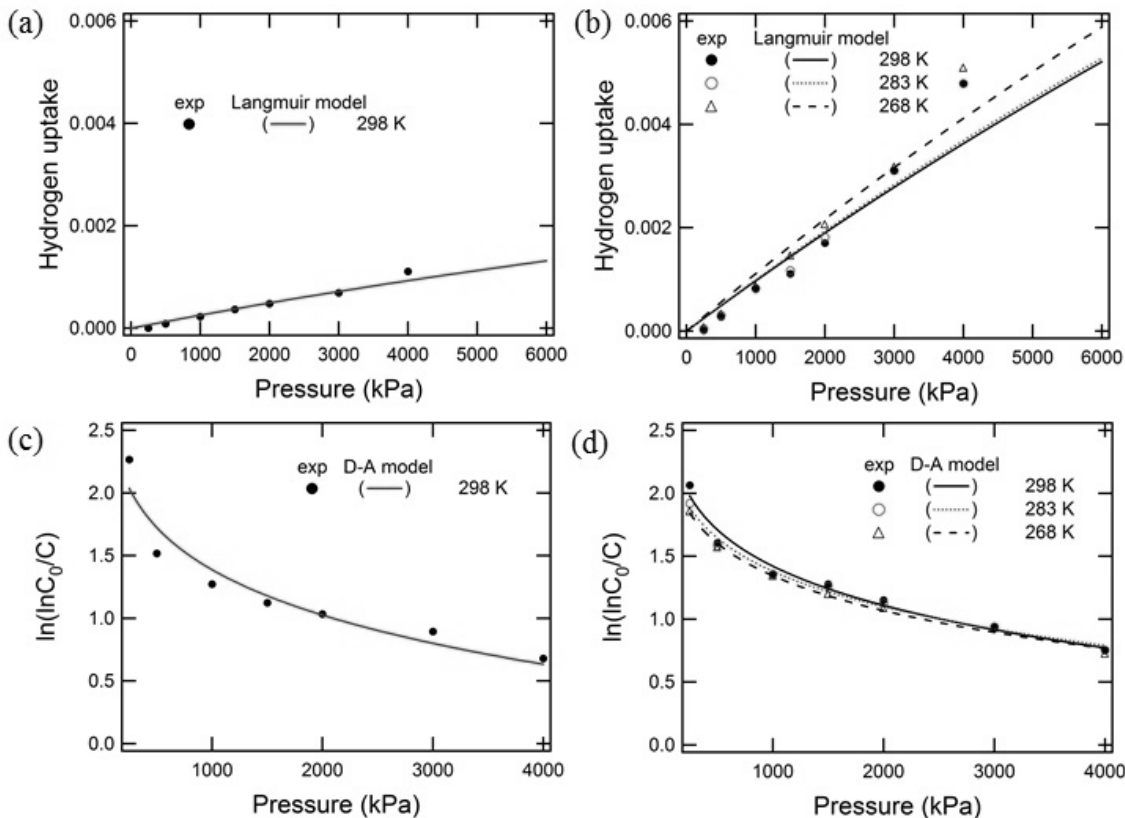


Figure 6 Langmuir model and experimental results for: (a) untreated low-rank coal; (b) activated carbon. D-A model and experimental results for: (c) untreated low-rank coal; (d) activated carbon. The fitting parameters are shown in Table 3. By employing both the Langmuir and D-A models for experimental data fitting, the correct parameters were obtained

This novel approximation is valid as long as the coupled parameter  $C_0$  is assumed to be similar in value, regardless of the isotherm model used. Figures 6c and 6d show that the range of our experimental results was sufficient to obtain correct fitting parameters. The fitting of the experimental results with the D-A model calculations shows very good agreement. The fitting parameters calculated from the results are shown in Table 3.

Table 3 shows that both  $C_0$ s for the activated carbon were much higher than the  $C_0$  for untreated low-rank carbon, as expected. This is because the total pore volume of the activated carbon is higher and the surface area larger than the untreated material. The activated carbon may have higher heterogeneity in its structure and energy, which indicates that the width of the particle size distribution of activated carbon is greater than that of the untreated carbon. The isosteric heat of adsorption ( $h_{st}$ ) of the activated carbon is also higher. This might be for the same reasons, that the total pore volume and surface area of the activated carbon were higher and larger than those of the untreated coal.

Table 3 Adsorption fitting parameters simultaneously obtained using the Langmuir and D-A models

Parameter	Untreated low-rank coal	Activated carbon
$C_0$	$(7.94 \pm 1.56) \times 10^{-3}$	$(40.17 \pm 1.56) \times 10^{-3}$
$h_{st}/R$ (K)	$536.02 \pm 4.05$	$778.30 \pm 30.27$
$k_0$ (1/kPa)	$(5.49 \pm 0.02) \times 10^{-6}$	$(1.79 \pm 0.03) \times 10^{-6}$
$E$ (J/mol)	$(170.37 \pm 0.62) \times 10^2$	$(149.46 \pm 0.31) \times 10^2$
$n$	$4.65 \pm 0.56$	$3.73 \pm 0.23$

### 4.3. Isosteric Heat of Adsorption

Figure 7 shows the pressure dependence of the isosteric heat of adsorption plotted using Equation 6 with the parameters obtained in Table 3. The boldest line corresponds to the untreated coal, while the other lines correspond to the activated carbon. The shape of the curves is quite similar.

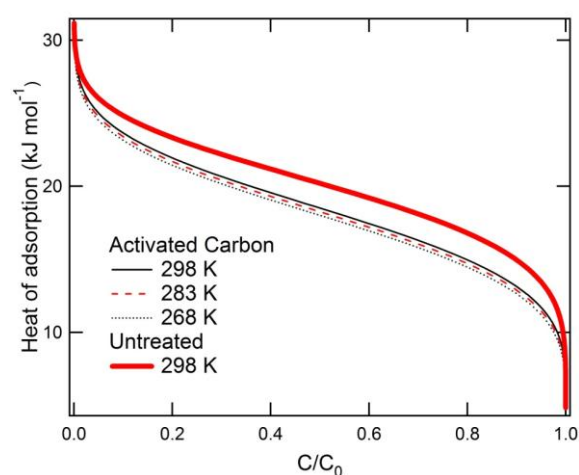


Figure 7 Uptake dependent of isosteric heat of adsorption for hydrogen on activated carbon using Equation 4 at 268 K, 283 K and 298 K, compared with untreated coal at 298 K

In general, the isosteric heat of adsorption decreases at higher vapor uptake. The adsorption of hydrogen is much faster at the initial and final stages of adsorption compared to the intermediate stage. This is attributed to the high value of parameter  $n$ , which is around 3.73. For

microporous carbon, this value is as expected (Choma et al., 1993). However, according to Dubinin (1975), his model captures adsorption with ideal micropores which have a size of around 0.7 nm. The average pore size of the activated carbon in this study is around 1.2 nm, which is hardly an ideal micropore. Therefore, it is safe to say that there are smaller pores which meet the defined micropore size, and there also exist larger ones whose size is at the boundary between the definition of micropores and mesopores (around 1.2 nm to 2 nm or larger).

In this sense, the physical explanation of the results can be made using several stages. At the initial stage, the difference is profound. For activated carbon, the hydrogen may be adsorbed rapidly into smaller micropores which reside inside larger micropores and/or mesopores. This produces a stronger interaction between hydrogen and the activated carbon surface (Figure 8). In addition, the heterogeneous pore sizes also lead to the non-uniform adsorption rate, which can be seen in the narrower intermediate stage compared to the untreated coal. On the other hand, with regard to the untreated coal, at the initial stage the hydrogen may not be adsorbed as rapidly as with the activated carbon, and the intermediate stage is broader than with the activated carbon, which reflects a lower heterogeneity value. The final stages for the two samples are more or less similar.

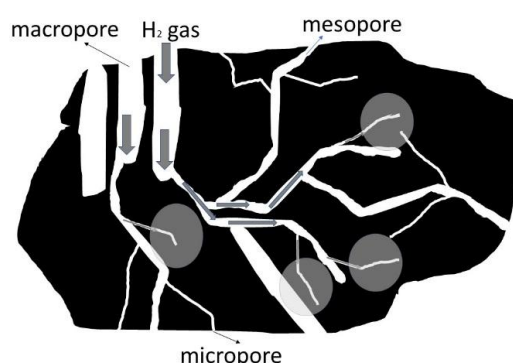


Figure 8 Schematic illustration of the hydrogen adsorption mechanism on the activated carbon surface. At the initial stage of adsorption, hydrogen gas is rapidly adsorbed in the relatively smaller micropores which reside in the larger micropores and/or mesopores (indicated by the grey circles)

## 5. CONCLUSION

Activated carbon has been produced from untreated Indonesian low-rank coal using a ball mill mechano-chemical method and its adsorption parameters have been successfully calculated using a coupled Langmuir and D-A isotherm model. It was found that the activated carbon has a higher pore volume and larger surface area than the low-rank coal. This leads to a higher hydrogen uptake or saturated amount of adsorbed hydrogen in the activated carbon compared to the untreated coal. The saturated hydrogen adsorption capacity of activated carbon led to an increase of about 500%, from 0.8% to 4.02%. From the calculation using the coupled Langmuir and D-A models, it is observed that the heterogeneity of energy distribution (which is related to the width of pore size distribution) of the activated carbon structure slightly increases, as shown by the  $n$  parameter, which is lower than that of untreated coal. It was found that the isosteric heat of adsorption increases rapidly at the initial and final stages of adsorption due to the adsorption of hydrogen on smaller micropores which reside inside larger ones.

## 6. ACKNOWLEDGEMENT

The publication of this article is supported by the United States Agency for International Development (USAID) through the Sustainable Higher Education Research Alliance (SHERA)

Program for the Universitas Indonesia Scientific Modeling, Application, Research and Training for City-centered Innovation and Technology (SMART CITY) Project, Grant #AID-497-A-1600004, Sub Grant #IIE-00000078-UI-1. Comprehensive discussions with and comments from Dr.-Ing. Nasruddin of the Department of Mechanical Engineering, Universitas Indonesia, are very much appreciated.

## 7. REFERENCES

- Ahmadpour, A., Do, D.D., 1996. The Preparation of Active Carbons from Coal by Chemical and Physical Activation. *Carbon*, Volume 34(4), pp. 471–479
- Ahmadpour, A., Do, D.D., 1997. The Preparation of Activated Carbon from Macadamia Nutshell by Chemical Activation. *Carbon*, Volume 35(12), pp. 1723–1732
- Ahn, D.H., Gibbs, B.M., Ko, K.H., Kim, J.J., 2001. Gasification Kinetics of an Indonesian Sub-bituminous Coal-Char with CO<sub>2</sub> at Elevated Pressure. *Fuel*, Volume 80(11), pp. 1651–1658
- Baheti, V., Naeem, S., Militky, J., Okrasa, M., Tomkova, B., 2015. Optimized Preparation of Activated Carbon Nanoparticles from Acrylic Fibrous Wastes. *Fibers and Polymers*, Volume 16(10), pp. 2193–2201
- Bouchelta, C., Medjram, M.S., Bertrand, O., Bellat, J.P., 2008. Preparation and Characterization of Activated Carbon from Date Stones by Physical Activation with Steam. *Journal of Analytical and Applied Pyrolysis*, Volume 82(1), pp. 70–77
- Caturla, F., Molina-Sabio, M., Rodriguez-Reinoso, F., 1991. Preparation of Activated Carbon by Chemical Activation with ZnCl<sub>2</sub>. *Carbon*, Volume 29(7), pp. 999–1007
- Chakraborty, A., Saha, B.B., Koyama, S., Ng, K.C., 2006. On the Thermodynamic Modeling of the Isotheric Heat of Adsorption and Comparison with Experiments. *Applied Physics Letters*, Volume 89(17), pp.171901-1–171901-3
- Chambers, A., Park, C., Baker, R.T.K., Rodriguez, N.M., 1998. Hydrogen Storage in Graphite Nanofibers. *The Journal of Physical Chemistry B*, Volume 102(22), pp. 4253–4256
- Choma, J., Burakiewicz-Mortka, W., Jaroniec, M., Gilpin R.K., 1993. Studies of the Structural Heterogeneity of Microporous Carbons using Liquid/Solid Adsorption Isotherms. *Langmuir*, Volume 9(10), pp. 2555–2561
- De la Casa-Lillo, M.A., Lamari-Darkrim, F., Cazorla-Amorós, D., Linares-Solano, A., 2002. Hydrogen Storage in Activated Carbons and Activated Carbon Fibers. *The Journal of Physical Chemistry B*, Volume 106(42), pp. 10930–10934
- Dubin, M.M., 1975. In *Progress in Membrane and Surface Science*. In Cadenhead, D.A. (Ed.), Volume 9, Chapter 1, pp. 1–70, Academic Press, New York
- Do, D.D., 1998. *Adsorption Analysis: Equilibria and Kinetics*, Imperial College Press, London, pp. 49–84
- Dong, J., Wang, X., Xu, H., Zhao, Q., Li, J., 2007. Hydrogen Storage in Several Microporous Zeolites. *International Journal of Hydrogen Energy*, Volume 32(18), pp. 4998–5004
- Elias, D.C., Nair, R.R., Mohiuddin, T.M.G., Morozov, S.V., Blake, P., Halsall, M.P., Ferrari, A.C., Boukhvalov, D.W., Katsnelson, M.I., Geim, A.K., Novoselov, K.S., 2009. Control of Graphene's Properties by Reversible Hydrogenation: Evidence for Graphene. *Science*, Volume 323(5914), pp. 610–613
- El Qada, E.N., Allen, S.J., Walker, G.M., 2006. Adsorption of Methylene Blue onto Activated Carbon Produced from Steam Activated Bituminous Coal: A Study of Equilibrium Adsorption Isotherm. *Chemical Engineering Journal*, Volume 124(1-3), pp. 103–110
- Gil, A., Korili, S.A., 2000. Structural Heterogeneity of Microporous Materials from Nitrogen Adsorption at 77 K. *Boletín de la Sociedad Española de Cerámica y Vidrio*, Volume 39(4), pp. 535–539

- Harjanto, S., Yuniar, S.W., Chodijah, S., Nasruddin, 2013. Hydrogen Adsorption Behavior of Mechanically Milled and Pelletized Coconut Shell Activated Carbon. *Material Science Forum*, Volume 737, pp. 98–104
- Hu, Y.H., Ruckenstein, E., 2006. Applicability of Dubinin-Astakhov Equation to CO<sub>2</sub> Adsorption on Single-walled Carbon Nanotubes. *Chemical Physics Letters*, Volume 425(4-6), pp. 306–310
- Ioannidou, O., Zabaniotou, A., 2007. Agricultural Residues as Precursors for Activated Carbon Production—A Review. *Renewable and Sustainable Energy Reviews*, Volume 11(9), pp. 1966–2005
- Jaroniec, M., 1995. *Characterization of Nanoporous Materials*. In Pinnavaia, T.J. and Thorpe, M.F. (Ed), *Access in Nanoporous Materials*, pp. 255–272, Plenum Press, New York
- Jiménez, V., Sánchez, P., Díaz, J.A., Valverde, J.L., Romero, A., 2010. Hydrogen Storage Capacity on Different Carbon Materials. *Chemical Physics Letters*, Volume 485(1-3), pp. 152–155
- Kumamoto, S., Takahashi, Y., Ishibashi, K., Noda, Y., Yamada, K., Chida, T., 1994. Production of Activated Carbon for Utilization of Bark from Russian Wood. *Transaction Material Research Society Japan*, Volume 18A (Ecomaterials), pp. 647–650
- Lee, H., Lee, J.W., Kim, D.Y., Park, J., Seo, Y.T., Zeng, H., Moudrakovski, I.L., Ratcliffe, C.I., Ripmeester, J.A., 2005. Tuning Clathrate Hydrates for Hydrogen Storage. *Nature*, Volume 434, pp. 743–746
- Li, H., Eddaoudi, M., O’Keeffe, M., Yaghi, O.M., 1999. Design and Synthesis of an Exceptionally Stable and Highly Porous Metal-Organic Framework. *Nature*, Volume 402(6759), pp. 276–279
- Limousin, G., Gaudet, J.P., Charlet, L., Szenknect, S., Barthes, V., Krimissa, M., 2007. Sorption Isotherms: A Review on Physical Bases, Modeling and Measurement. *Applied Geochemistry*, Volume 22(2), pp. 249–275
- Marsh, H., Yan, D.S., O’Grady, T.M., Wennerberg, A., 1984. Formation of Active Carbons from Cokes using Potassium Hydroxide. *Carbon*, Volume 22(6), pp. 603–611
- Martin, A., Loh, W.S., Rahman, K.A., Thu, K., Surayawan, B., Alhamid, M.I., Ng, K.C., 2011. Adsorption Isotherms of CH<sub>4</sub> on Activated Carbon from Indonesian Low Grade Coal. *Journal of Chemical & Engineering Data*, Volume 56(3), pp. 361–367
- Moreno-Castilla, C., Carrasco-Marín, F., López-Ramón, M.V., Alvarez-Merino, M.A., 2001. Chemical and Physical Activation of Olive-Mill Waste Water to Produce Activated Carbons. *Carbon*, Volume 39(9), pp. 1415–1420
- Nandi, M., Okada, K., Dutta, A., Bhaumik, A., Maruyama, J., Derks, D., Uyama, H., 2012. Unprecedented CO<sub>2</sub> Uptake over Highly Porous N-doped Activated Carbon Monoliths Prepared by Physical Activation. *Chemical Communications*, Volume 48(83), pp. 10283–10285
- Nasruddin, N., Kosasih, E.A., Kurniawan, B., Supriyadi, S., Zulkarnain, I.A., 2016. Optimization of Hydrogen Storage Capacity by Physical Adsorption on Open-ended Single-walled Carbon Nanotube as Diameter Function. *International Journal of Technology*, Volume 7(2), pp. 264–273
- Niemann, U.M., Srinivasan, S.S., Phani, A.R., Kumar, A., Goswami, D.Y., Stefanakos, E.K., 2008. Nanomaterials for Hydrogen Storage Applications: A Review. *Journal of Nanomaterials*, Volume 2008, pp. 1–9
- Nor, N.M., Sukri, M.F.F., Mohamed, A.R., 2016. Development of High Porosity Structures of Activated Carbon via Microwave-assisted Regeneration for H<sub>2</sub>S Removal. *Journal of Environmental Chemical Engineering*, Volume 4(4), pp. 4839–4845
- Schlapbach, L., Züttel, A., 2001. Hydrogen-storage Materials for Mobile Applications. *Nature*, Volume 414(6861), pp. 353–358

- Sekirifa, M.L., Hadj-Mahammed, M., Pallier, S., Baameur, L., Richard, D., Al-Dujaili, A.H., 2013. Preparation and Characterization of an Activated Carbon from a Date Stones Variety by Physical Activation with Carbon Dioxide. *Journal of Analytical and Applied Pyrolysis*, Volume 99, pp. 155–160
- Serrano, E., Guillermo, R., Javier, G.M., 2009. Nanotechnology for Sustainable Energy. *Renewable and Sustainable Energy Reviews*, Volume 13(9), pp. 2373–2384
- Stoeckli, F., Jakubov, T., Lavanchy, A., 1994. Water Adsorption in Active Carbons Described by the Dubinin-Astakhov Equation. *Journal of the Chemical Society, Faraday Transaction*, Volume 90(5), pp. 783–786
- Sudibandriyo, M., Wulan, P.P., Prasodjo, P., 2015. Adsorption Capacity and Its Dynamic Behavior of the Hydrogen Storage on Carbon Nanotubes. *International Journal of Technology*, Volume 6(7), pp. 1128–1136
- Tsai, W.T., Chang, C.Y., Lee, S.L., 1998. A low Cost Adsorbent from Agricultural Waste Corn Cob by Zinc Chloride Activation. *Bioresource Technology*, Volume 64(3), pp. 211–217
- Ushiki, I., Ota, M., Sato, Y., Inomata, H., 2013. Measurement and Dubinin-Astakhov Correlation of Adsorption Equilibria of Toluene, Acetone, n-hexane, n-decane and Methanol Solutes in Supercritical Carbon Dioxide on Activated Carbon at Temperature from 313 to 353 K and at Pressure from 4.2 to 15.0 MPa. *Fluid Phase Equilibria*, Volume 344, pp. 101–107
- Viswanathan, B., Neel, P.I., Varadarajan, T.K., 2009. *Methods of Activation and Specific Applications of Carbon Materials*. National Centre of Catalysis Research, Indian Institute of Technology Madras, Chennai, India
- Welham, N.J., Berbenni, V., Chapman, P.G., 2002. Increased Chemisorption onto Activated Carbon After Ball-milling. *Carbon*, Volume 40(13), pp. 2307–2315
- Wu, F.C., Wu, P.H., Tseng, R.L., Juang, R.S., 2014. Description of Gas Adsorption Isotherms on Activated Carbons with Heterogeneous Micropores using the Dubinin-Astakhov Equation. *Journal of Taiwan Institute of Chemical Engineering*, Volume 45(4), pp. 1757–1763